Electronic Supplementary Material (ESI) for Journal of Materials Chemistry C.

Supplementary Information

Photoluminescence Study over Perovskite Materials Derived from Tungsten- and Lanthanide-Containing Aurivillius Layered Perovskite, $Bi_2Na_{0.63}Ln_{0.37}Ta_{1.75}W_{0.25}O_9$.

Keisuke Awaya,*[a] Ayaka Yamamoto,[b] Kazuto Hatakeyama,[c] and Shintaro Ida*[c]

a) Faculty of Advanced Science and Technology, Kumamoto University, 2-39-1, Kurokami, Chuo-ku, Kumamoto, 860-8555, Japan.

b) Graduate School of Science and Technology, Kumamoto University, 2-39-1, Kurokami, Chuo-ku, Kumamoto, 860-8555, Japan.

c) Institute of Industrial Nanomaterials (IINa), Kumamoto University, 2-39-1, Kurokami, Chuo-ku, Kumamoto, 860-8555, Japan.

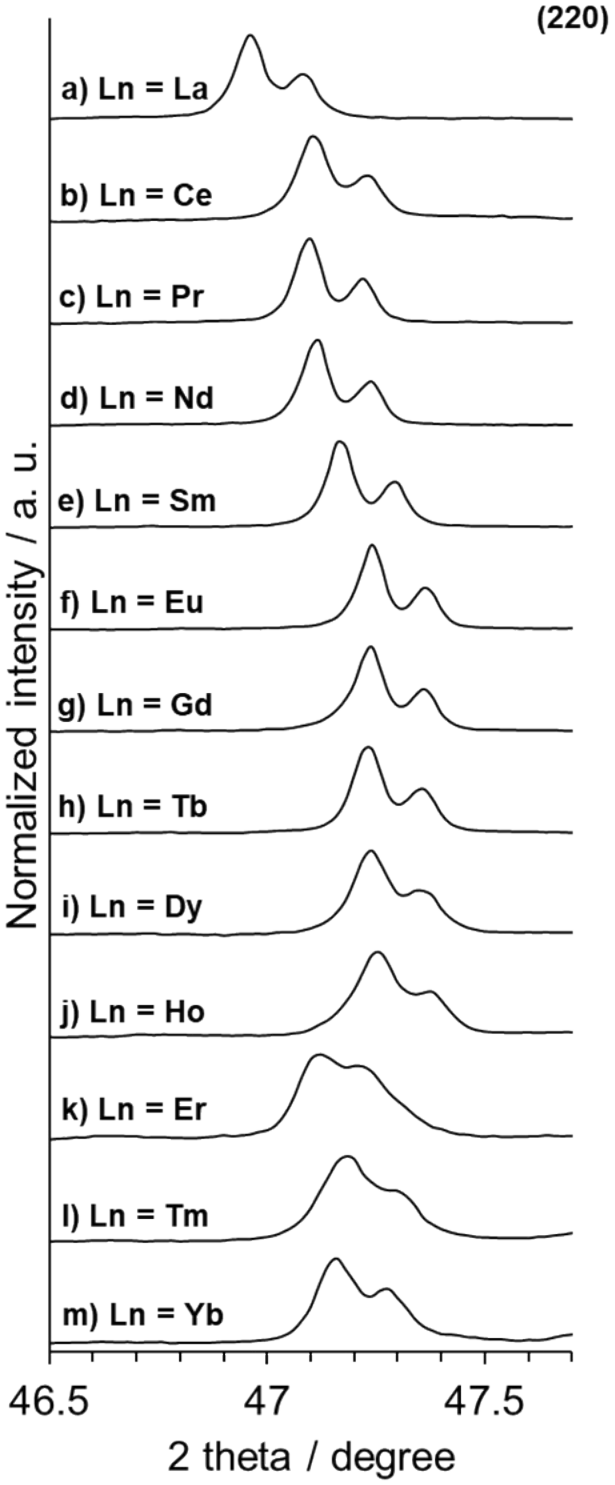

Figure S1. XRD pattern (2θ/θ scan, 2θ = 46.5-47.7 degrees) of $Bi_2Na_{0.63}Ln_{0.37}Ta_{1.75}W_{0.25}O_9$. Ln = (a) La, (b) Ce, (c) Pr, (d) Nd, (e) Sm, (f) Eu, (g) Gd, (h) Tb, (i) Dy, (j) Ho, (k) Er, (l) Tm, (m) Yb.

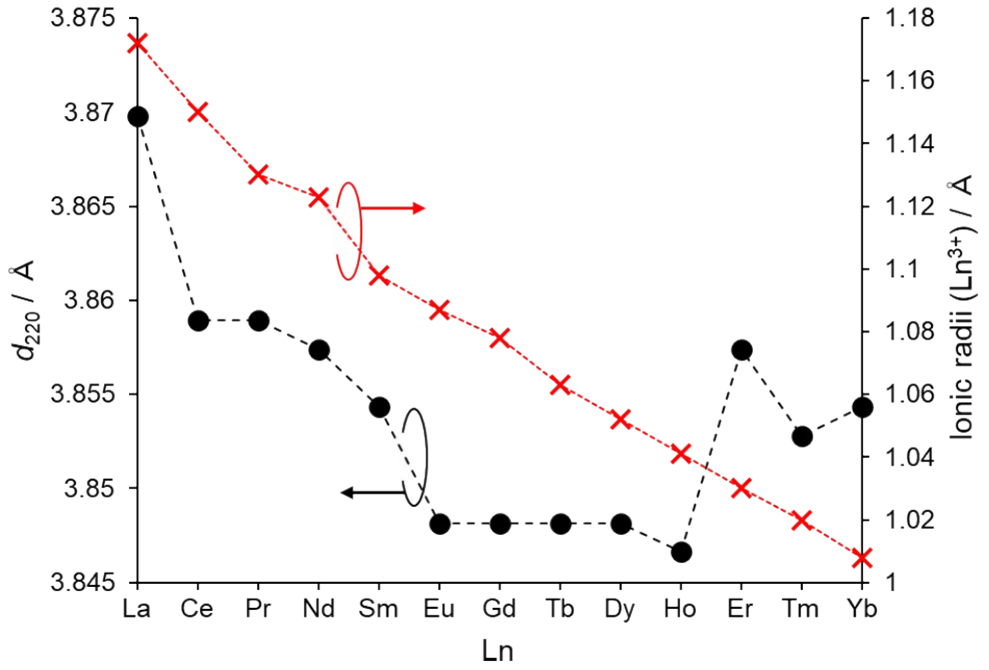

Figure S2. *d*-spacing values and ionic radii (Ln^{3+}) for (220) diffraction peak of $Bi_2Na_{0.63}Ln_{0.37}Ta_{1.75}W_{0.25}O_9$ (Ln = La-Yb).

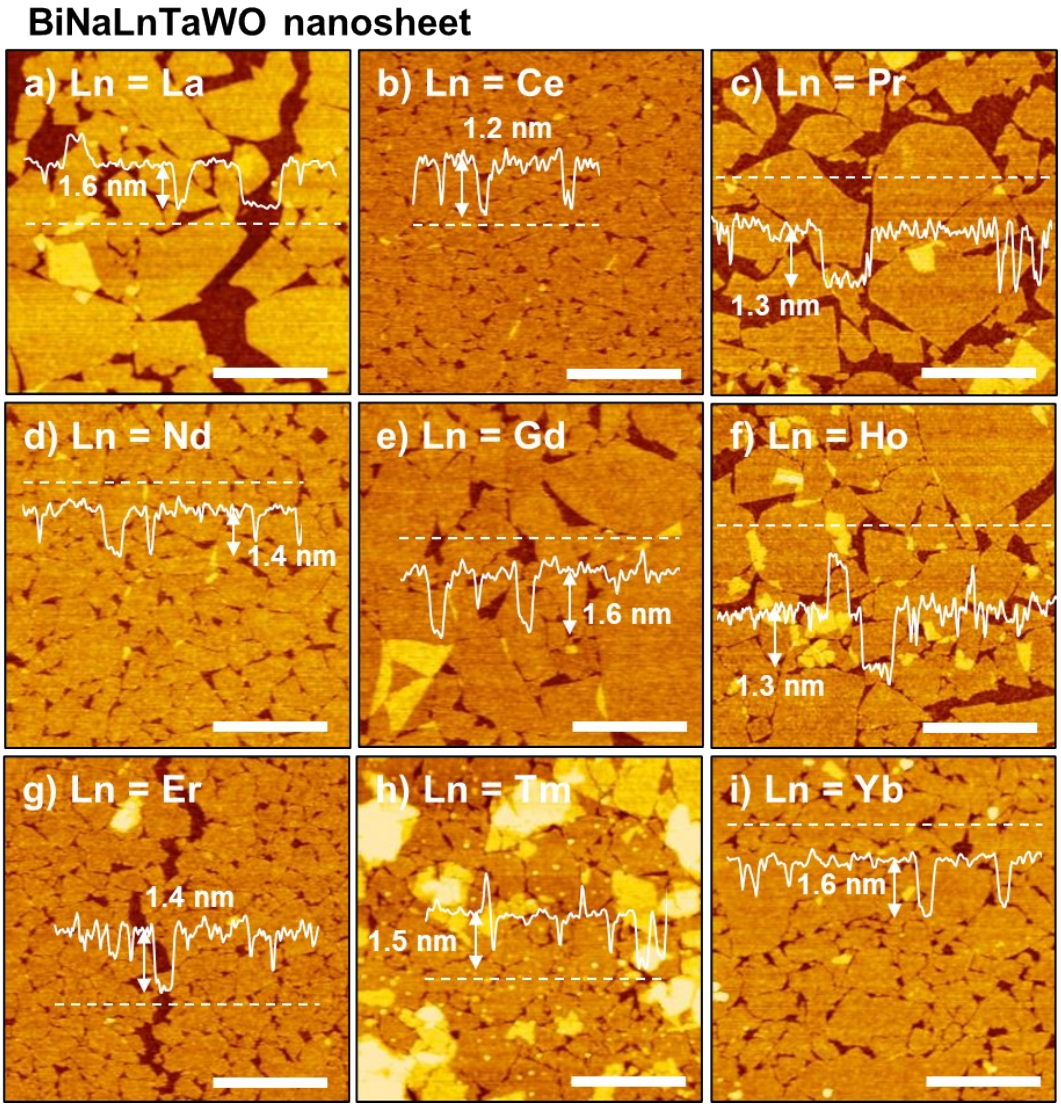

Figure S3. AFM images of BiNaLnTaWO nanosheet (Ln = (a) La, (b) Ce, (c) Pr, (d) Nd, (e) Gd, (f) Ho, (g) Er, (h) Tm, (i) Yb). Scale bar is 500 nm.

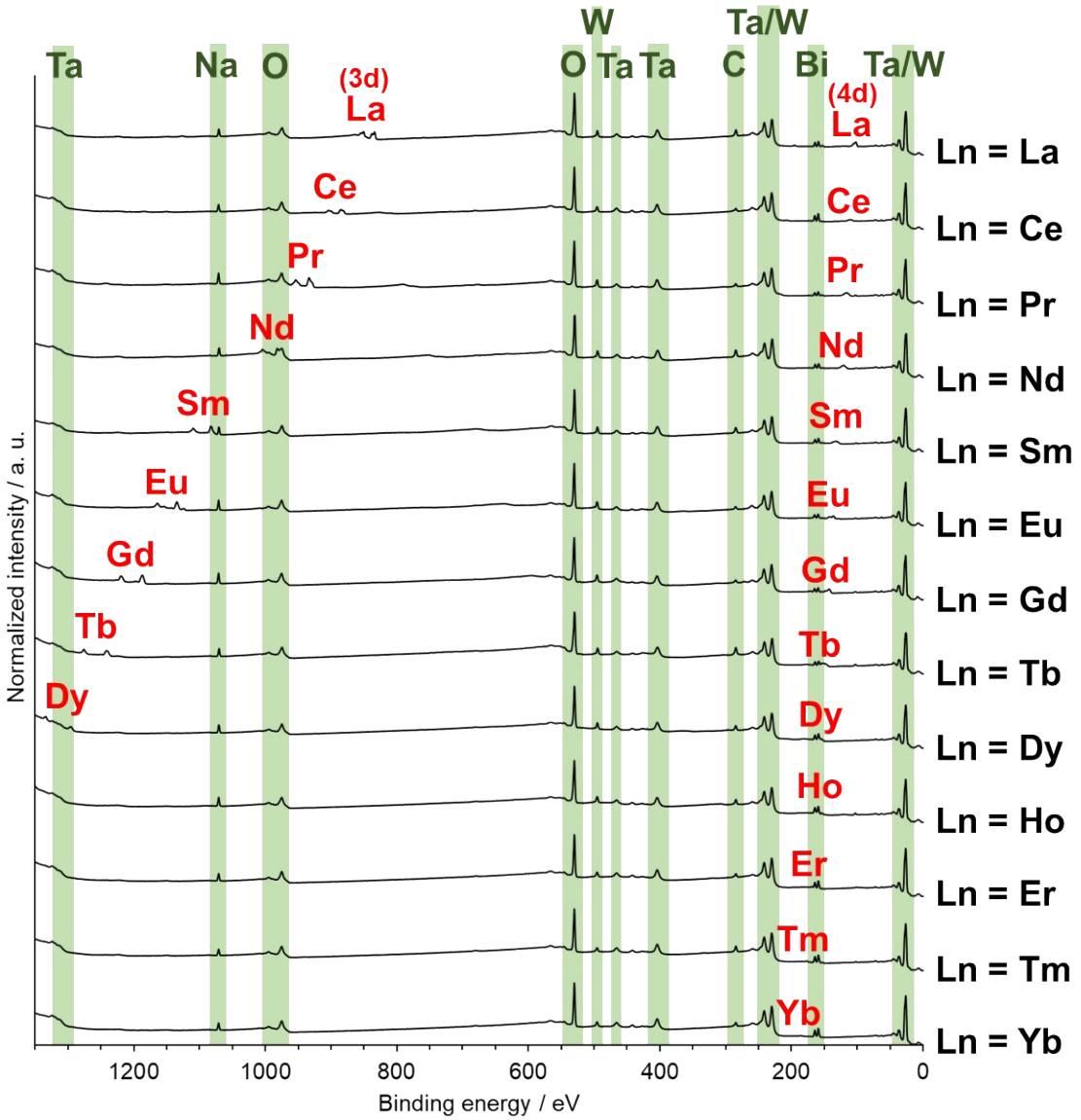

Figure S4. XPS survey scans (0-1350 eV) of BiNaLnTaWO nanosheet (Ln = La-Yb) spin-coating film on a quartz glass plate.

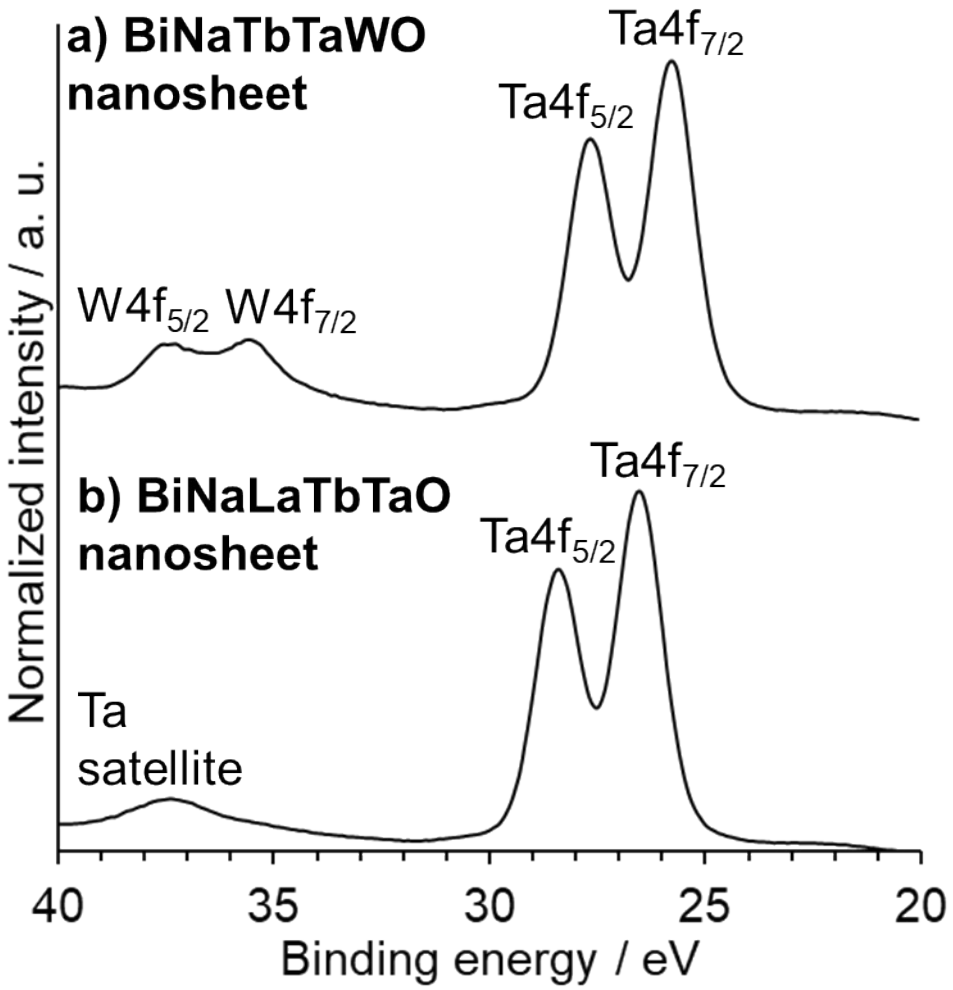

Figure S5. Ta 4f and W 4f XPS spectra of (a) BiNaTbTaWO and (b) BiNaLaTbTaO nanosheet spin-coating films on a quartz glass plate.

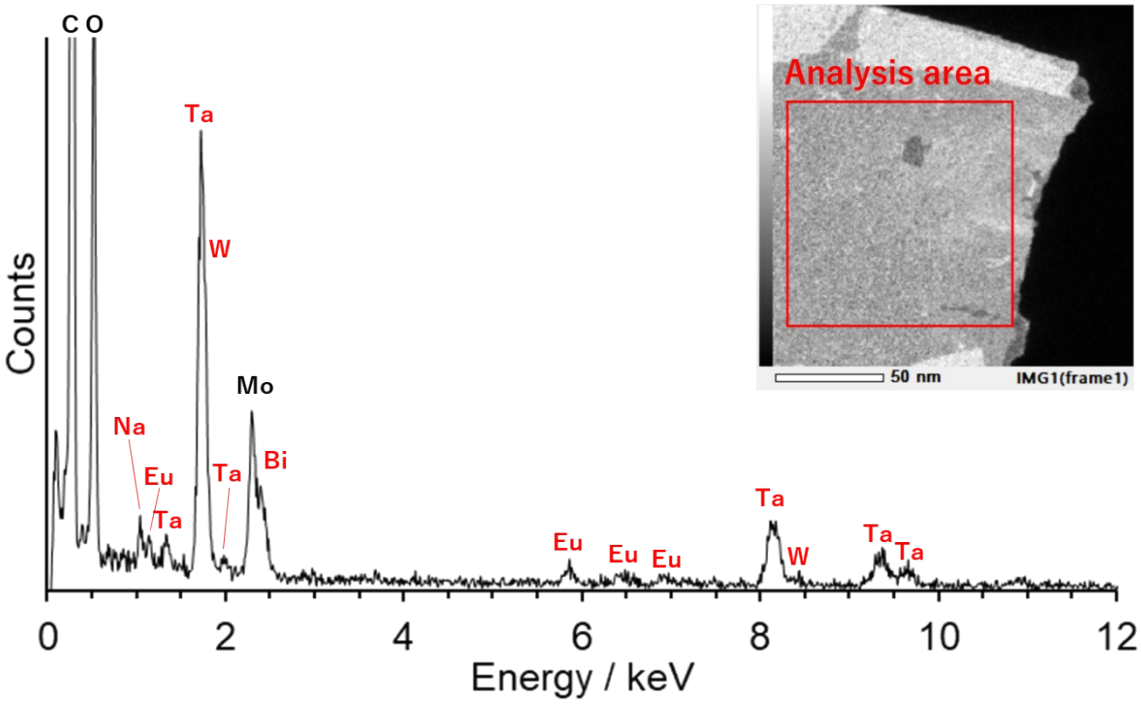

Figure S6. TEM-EDS spectra of BiNaEuTaWO nanosheet on a quantifoil Mo grid.

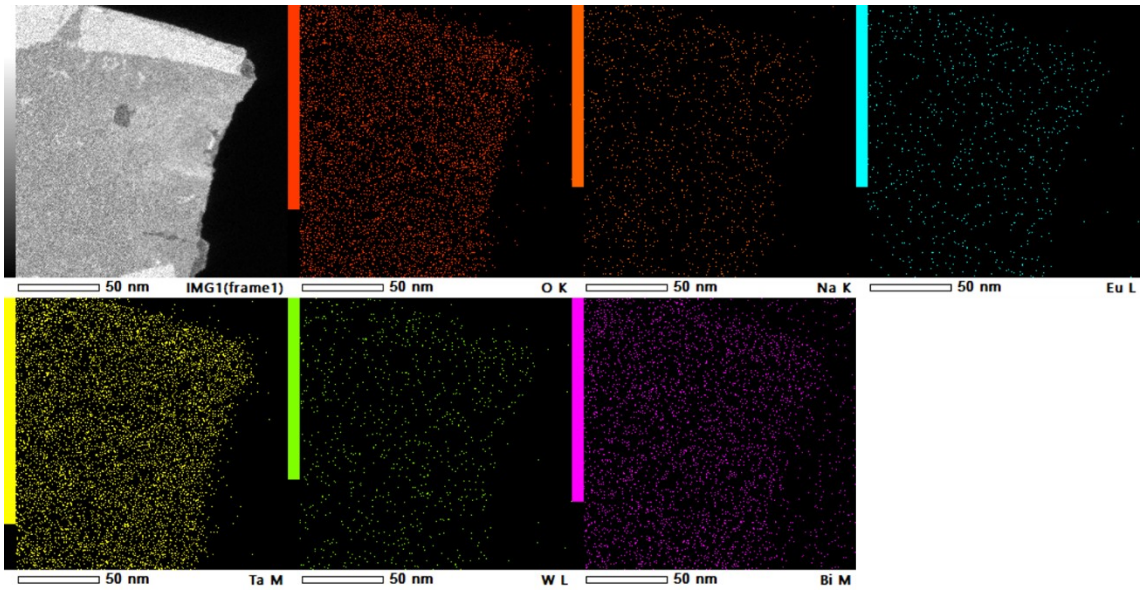

Figure S7. TEM-EDS mapping images of BiNaEuTaWO nanosheet on a quantifoil Mo grid.

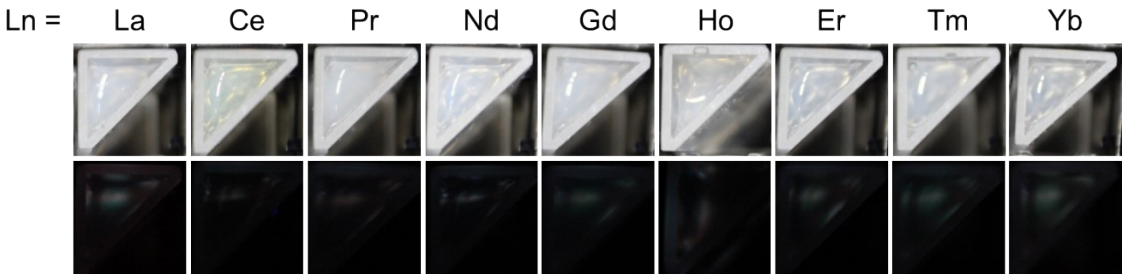

Figure S8. Photographs of BiNaLnTaWO nanosheet dispersing in 0.025 M TBAOH solution (Ln = La, Ce, Pr, Nd, Gd, Ho, Er, Tm, Yb; $\lambda_{ex.}$ = 280 nm).

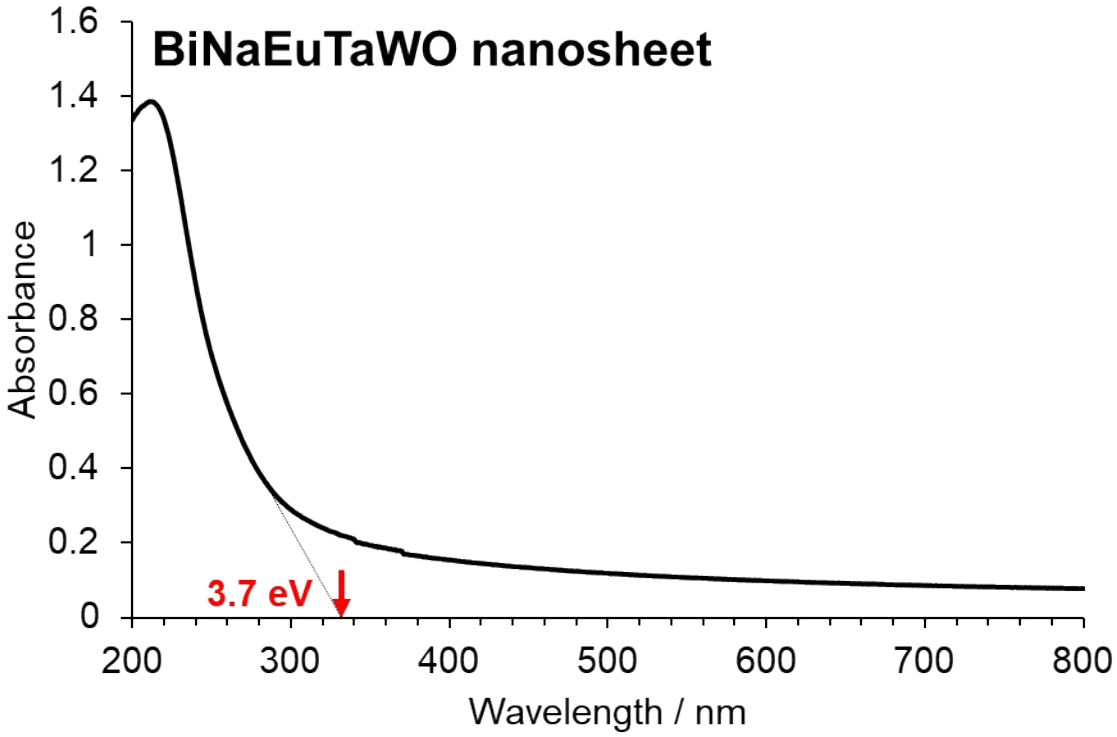

Figure S9. UV-Vis spectra of BiNaEuTaWO nanosheet spin-coating film on a quartz glass plate.

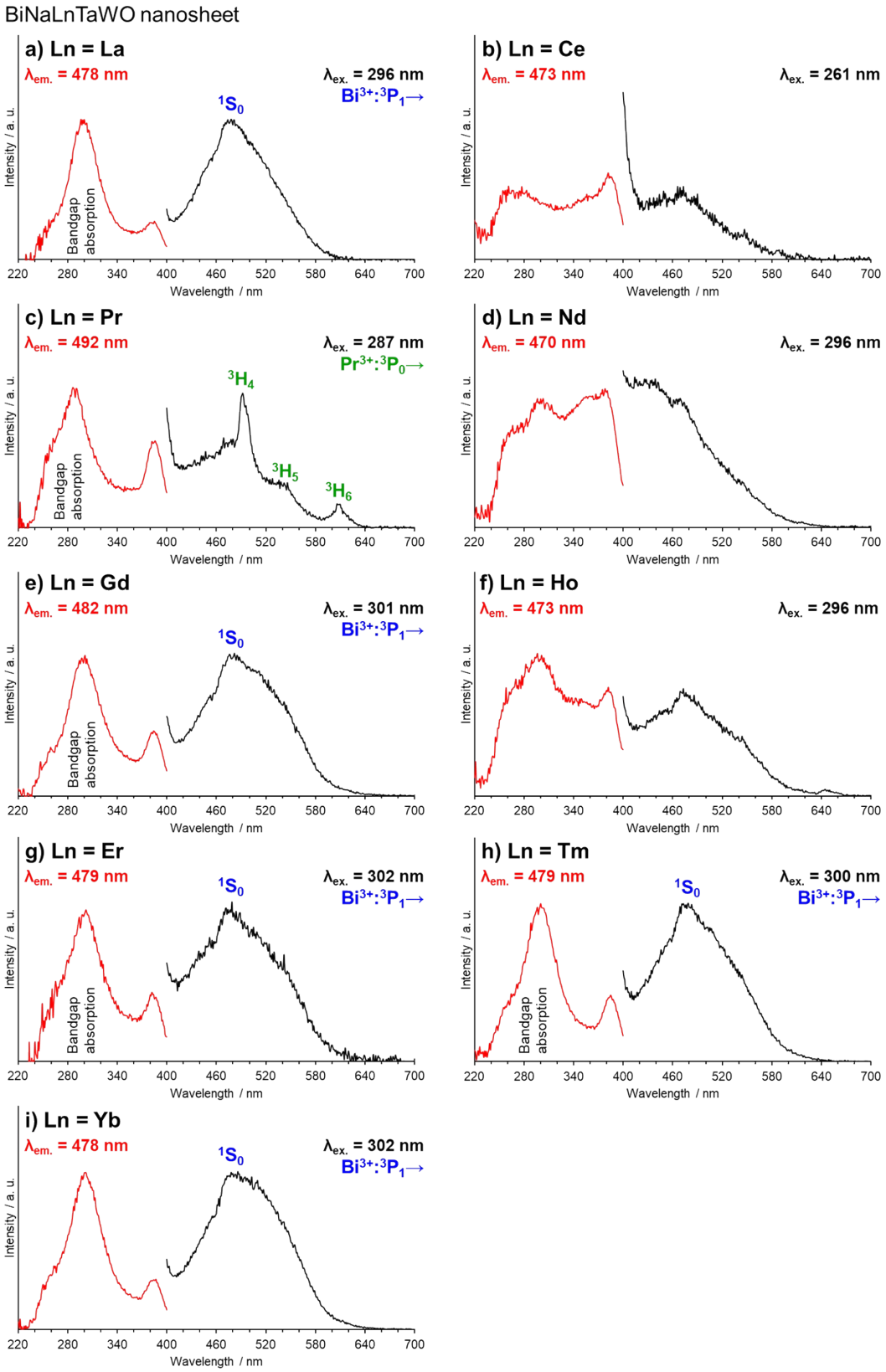

Figure S10. PL excitation and emission spectra of BiNaLnTaWO nanosheet dispersing in 0.025 M TBAOH solution (Ln = La, Ce, Pr, Nd, Gd, Ho, Er, Tm, Yb).

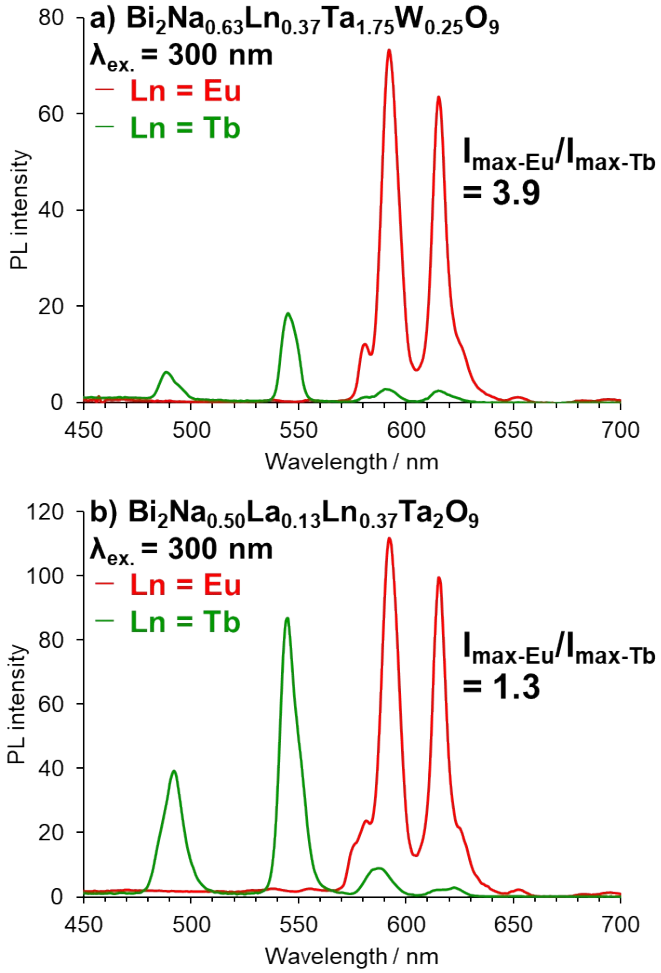

Figure S11. PL emission spectra (λ_{ex} = 300 nm) of $Bi_2Na_{0.63}Ln_{0.37}Ta_{1.75}W_{0.25}O_9$ and $Bi_2Na_{0.5}La_{0.13}Ln_{0.37}Ta_2O_9$; Ln = Eu or Tb)

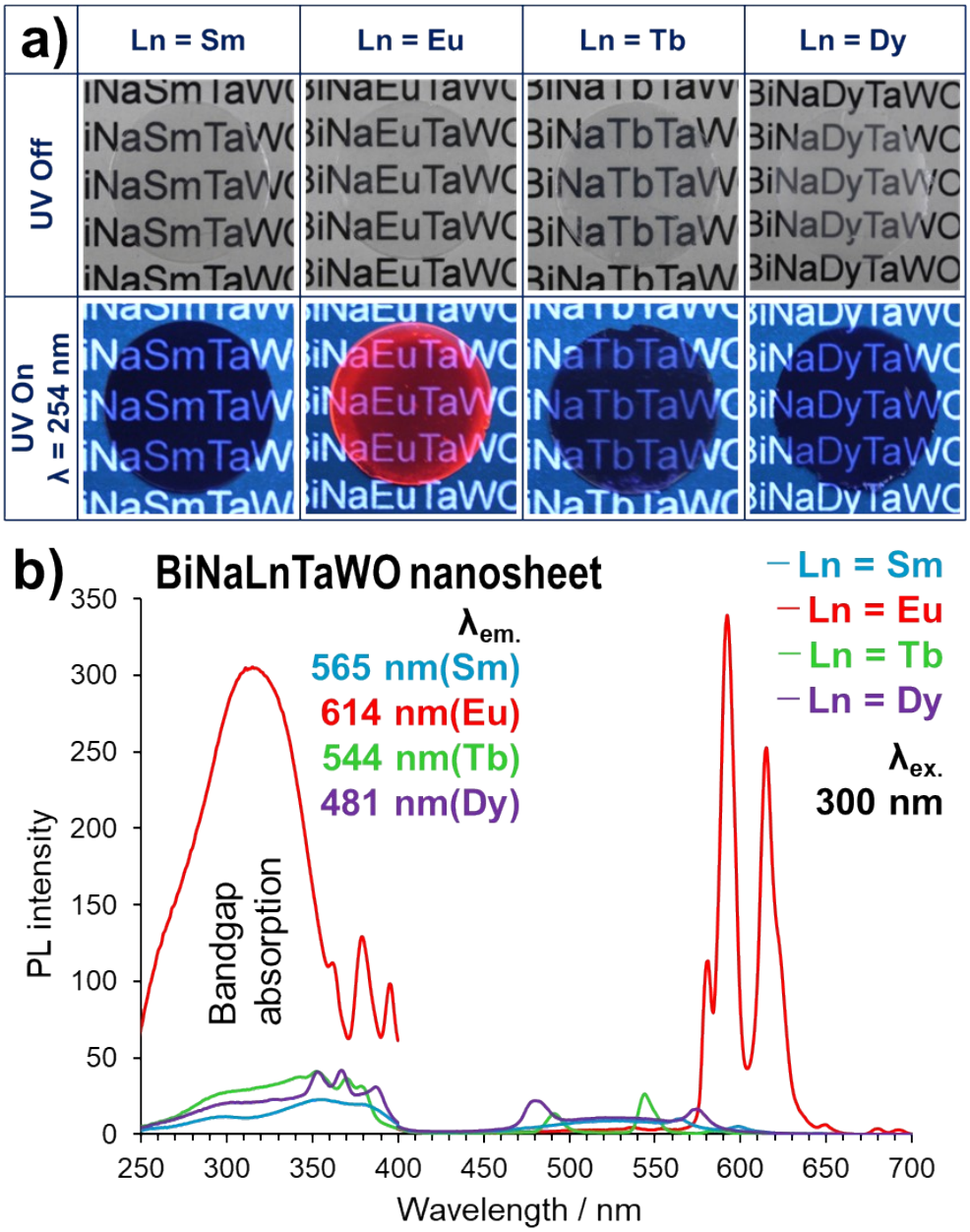

Figure S12. (a) Photographs of BiNaLnTaWO nanosheet free-standing films under UV-light illumination ($\lambda_{ex.}$ = 254 nm; Ln = Sm, Eu, Tb, Dy). (b) PL excitation ($\lambda_{em.}$ = 565 [Sm]; 614 [Eu]; 544 [Tb]; 481 nm [Dy]) and emission ($\lambda_{ex.}$ = 300 nm) spectra of BiNaLnTaWO nanosheet free-standing films.

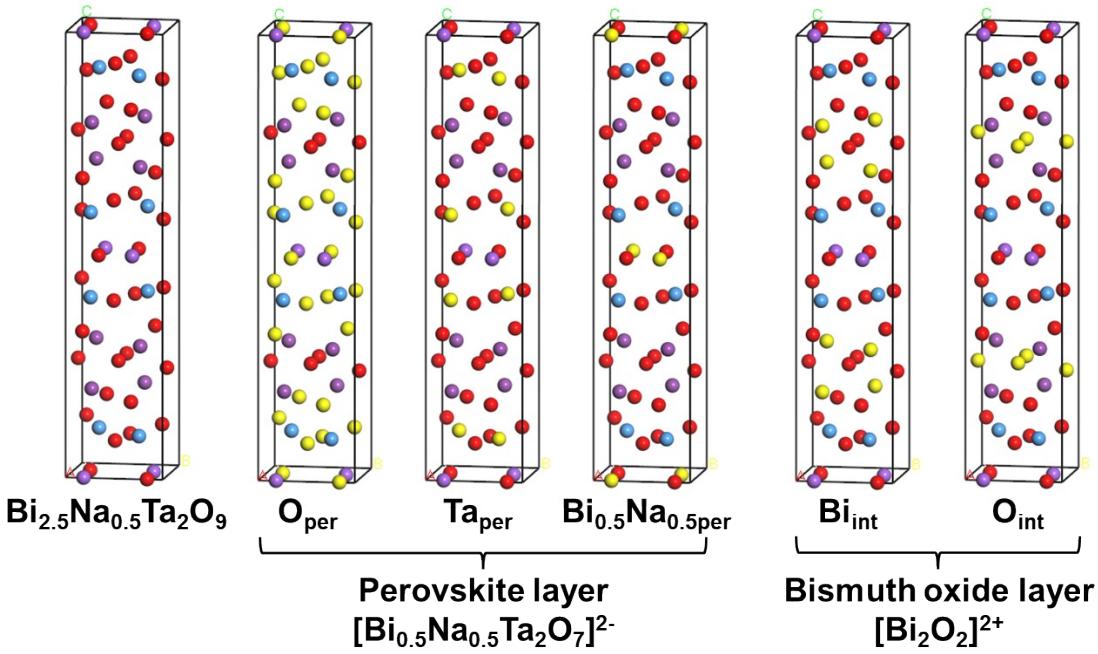

Figure S13. The unit cell of $Bi_{2.5}Na_{0.5}Ta_2O_9$ after geometry optimization using DFT calculation with the plane wave codes CASTEP. The denotations, "O_{per}", "Ta_{per}", "$Bi_{0.5}Na_{0.5per}$", "Bi_{int}", "O_{int}", are corresponded to the yellow-colored atoms in the unit cell.

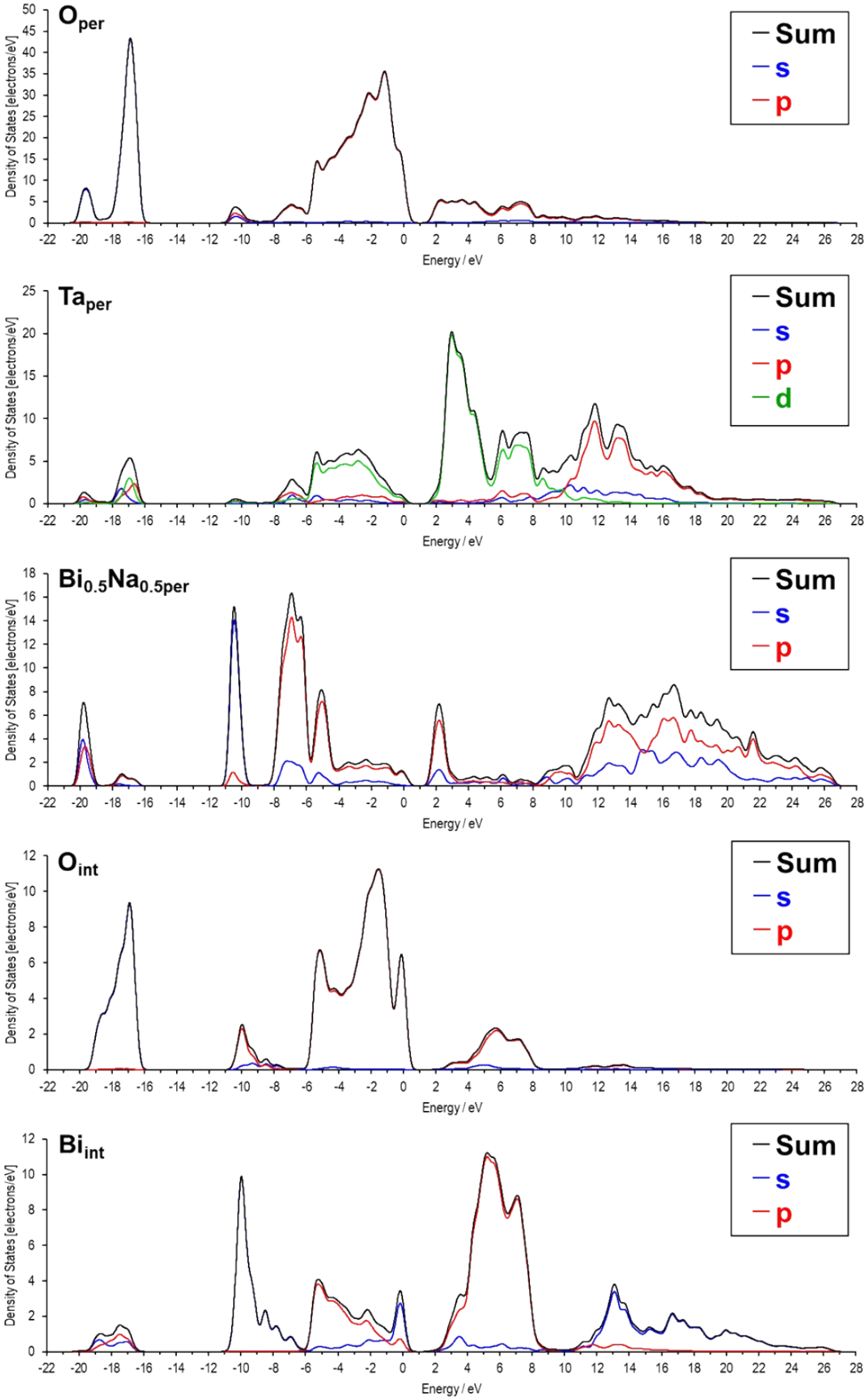

Figure S14. Partial density of states obtained from DFT calculation with the plane wave codes CASTEP. The denotations, "O_{per}", "Ta_{per}", "$Bi_{0.5}Na_{0.5per}$", "Bi_{int}", "O_{int}", are corresponded to yellow-colored atoms in the unit cell of $Bi_{2.5}Na_{0.5}Ta_2O_9$ in **Figure S11**.

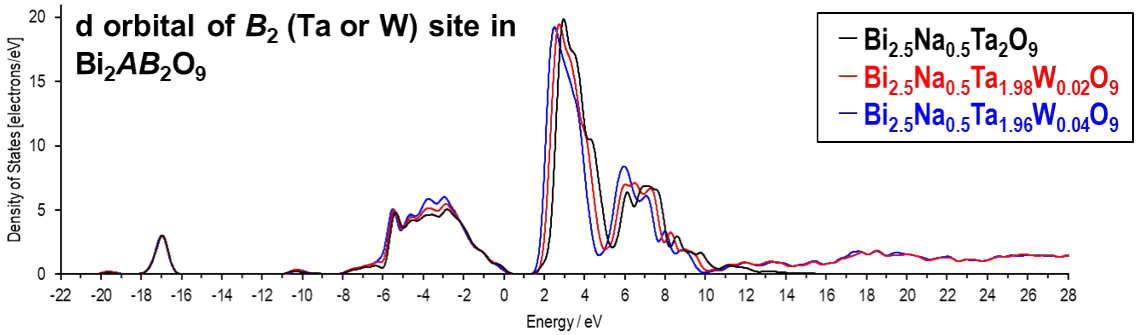

Figure S15. Partial density of states for d orbital of B_2 sites (Ta_2, $Ta_{1.98}W_{0.02}$, $Ta_{1.96}W_{0.04}$) of $Bi_{2.5}Na_{0.5}Ta_2O_9$, $Bi_{2.5}Na_{0.5}Ta_{1.98}W_{0.02}O_9$, and $Bi_{2.5}Na_{0.5}Ta_{1.96}W_{0.04}O_9$ obtained from DFT calculation with the plane wave codes CASTEP.

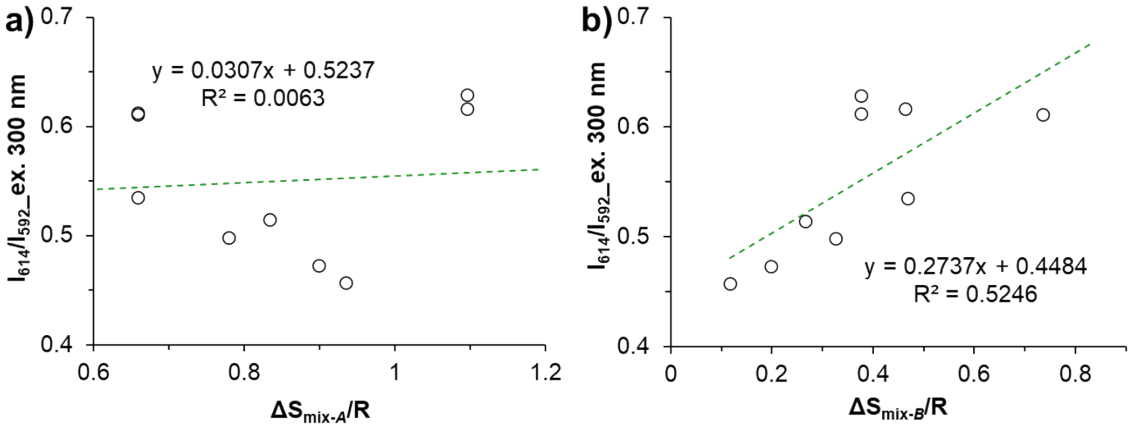

Figure S16. Relationship between structural entropy of the perovskite layer (A site: $\Delta S_{mix\text{-}A}$; B site: $\Delta S_{mix\text{-}B}$) of sample H1-H9 in Table 2 and PL emission ($\lambda_{ex.}$ = 300 nm) intensity ratio at 614 nm (Eu^{3+}, $^5D_0 \rightarrow {}^7F_2$ transition) over 592 nm (Eu^{3+}, $^5D_0 \rightarrow {}^7F_1$ transition).

Table S1. Summary of the chemical compositions and PL properties of BiNaEuTaWO nanosheet in the present work and various perovskite nanosheets reported in the previous literatures.

Chemical composition of perovskite nanosheet*[a]	Luminescent centre	Quantum yield / % ($\lambda_{ex.}$)	I_{7F2}/I_{7F1} ratio (for Eu^{3+} only)	Phase of the starting layered perovskite*[b]	Ref. No.
$Eu_{0.56}Ta_2O_7$	Eu^{3+}	-	1.0	RP ($Li_2A_{2/3}B_2O_7$)	S1
$Gd_{1.4}Eu_{0.6}Ti_3O_{10}$	Eu^{3+}	3.3 (245 nm)	4.5	RP ($K_2A_2B_3O_{10}$)	S2
$Gd_{1.4}Tb_{0.6}Ti_3O_{10}$	Tb^{3+}*[c]	-	-	RP ($K_2A_2B_3O_{10}$)	
$La_{0.95}Eu_{0.05}Ta_2O_7$	Eu^{3+}	-	-	DJ ($RbAB_2O_7$)	
$La_{0.7}Tb_{0.3}Ta_2O_7$	Tb^{3+}	0.9 (230 nm)	-	DJ ($RbAB_2O_7$)	
$La_{0.90}Eu_{0.05}Nb_2O_7$	Eu^{3+}	-	3.8	DJ (KAB_2O_7)	S3
$Ca_{1.9}Tb_{0.1}Ta_3O_{10}$	Tb^{3+}	~19 (270 nm)	-	DJ ($CsA_2B_3O_{10}$)	S4
$Bi_{0.16}Sr_{0.75}Ta_2O_7$	Bi^{3+}	-	-	AU ($Bi_2AB_2O_9$)	S5
$Bi_{0.06}Ca_{0.64}Ta_2O_{7-\delta}$	Bi^{3+}	-	-	AU ($Bi_2AB_2O_9$)	S6
$Bi_{0.05}Na_{0.34}Ta_2O_{7-\delta}$	Bi^{3+}	-	-	AU ($Bi_2AB_2O_9$)	
$Bi_{0.11}La_{0.05}Na_{0.22}Ta_2O_{7-\delta}$	Bi^{3+}	0.05 (280 nm)	-	AU ($Bi_2AB_2O_9$)	S7
$Bi_{0.11}Sm_{0.07}Na_{0.26}Ta_2O_{7-\delta}$	Bi^{3+} & Sm^{3+}	-	-	AU ($Bi_2AB_2O_9$)	
$Bi_{0.12}Eu_{0.06}Na_{0.20}Ta_2O_{7-\delta}$	Bi^{3+} & Eu^{3+}	-	0.6	AU ($Bi_2AB_2O_9$)	
$Bi_{0.11}Tb_{0.07}Na_{0.23}Ta_2O_{7-\delta}$	Bi^{3+} & Tb^{3+}	-	-	AU ($Bi_2AB_2O_9$)	
$Bi_{0.10}Dy_{0.05}Na_{0.22}Ta_2O_{7-\delta}$	Bi^{3+} & Dy^{3+}	-	-	AU ($Bi_2AB_2O_9$)	
$Bi_{0.04}Na_{0.63}Eu_{0.32}Ta_{1.50}W_{0.09}O_{7-\delta}$	Eu^{3+}	0.17 (310 nm)	1.1	AU ($Bi_2AB_2O_9$)	This work
$Bi_{0.04}Na_{0.63}Tb_{0.34}Ta_{1.63}W_{0.09}O_{7-\delta}$	Tb^{3+}*[c]	-	-	AU ($Bi_2AB_2O_9$)	

*a) The total molar charge of each nanosheet is ignored for the chemical composition.

*b) RP, DJ, and AU denote Ruddlesden-Popper, Dion-Jacobson, and Aurivillius phase layered perovskites, respectively.

*c) The luminescent centre exhibited very weak or no observable emission.

References

S1) T. C. Ozawa, K. Fukuda, K. Akatsuka, Y. Ebina, T. Sasaki, K. Kurashima and K. Kosuda, *J. Phys. Chem. C*, 2008, **112**, 1312-1315.

S2) S. Ida, C. Ogata, U. Unal, K. Izawa, T. Inoue, O. Altuntasoglu and Y. Matsumoto, *J. Am. Chem. Soc.*, 2007, **129**, 8956-8957.

S3) T. C. Ozawa, K. Fukuda, K. Akatsuka, Y. Ebina and T. Sasaki, *Chem. Mater.*, 2007, **19**, 6575-6580.

S4) S. Ida, S. Koga, T. Daio, H. Hagiwara, T. Ishihara, *Angew. Chem.* 2014, **126**, 13294-13298.

S5) S. Ida, C. Ogata, M. Eguchi, W. J. Youngblood, T. E. Mallouk and Y. Matsumoto, *J. Am. Chem. Soc.*, 2008, **130**, 7052-7059.
S6) K. Awaya and S. Ida, *Chem. Mater.*, 2023, **35**, 3713-3721.
S7) K. Awaya, K. Hatakeyama and S. Ida, *Adv. Opt. Mater.*, 2024, **12**, 2301228.